Delay line readout of a large dimension multi-wire proportional chamber[*]

LI Xian-Li(黎先利)[1,2;1]   ZHANG Yun-Long(张云龙)[1]   QIAN Hao(钱浩)[1]

XU Zi-Zong(许咨宗)[1]   WANG Xiao-Lian(汪晓莲)[1;2]

[1] University of Science and Technology of China, Hefei 230026, China
[2] Northwest Institute of Nuclear Technology, Xi'an 710613, China

Abstract: A two dimensional multi-wire proportional chamber with delay line readout was developed, which has a large sensitive area of 30 cm×30 cm. Two cathode planes using printed circuit boards are orthogonally placed to give two coordinates of the impact point of the particle. Signals collected from the cathode strips are amplified and discriminated from two ends of the delay line at each cathode board. By recording the time difference between the two discrimination pulses and the common gate pulse from anode wires, a coordinate position was reconstructed, and a position resolution of better than 1 mm could be obtained in the whole sensitive area along the anode wires.

Key words: MWPC, delay line, position resolution

PACS: 29.40.Cs, 29.40.Gx   **DOI:** 10.1088/1674-1137/36/6/007

1 Introduction

Multi-wire proportional chamber (MWPC), first proposed by Charpak in 1968, has proven to be a good choice as a position sensitive gas detector [1]. It is usually read out by the centroid finding method, the resistive charge division method and delay line readout. Among them, the centroid finding method has the best position sensing [2], but employs a large number of readout channels. Delay line readout is a simple and relatively accurate method for MWPC. It employs only two signal outputs for each coordinate and is more sensitive than the resistive charge division method.

A two dimensional position sensitive MWPC with delay line readout, which has a sensitive area of 30 cm×30 cm, was developed to track atmospheric muons. The sensitive volume of the detector is sealed by two cathodes made of printed circuit board. Each of the cathodes consists of three blocks: cathode strips, lumped delay line chips and front end amplifier electronics. The impact point where ionization takes place is determined by measuring the time delays of the current wave reaching the amplifier at each end of the delay line [3]. There are many successful delay wire chambers all over the world [2–5], but some problems still exist to construct a large delay wire chamber using cathode strips, such as the crosstalk and signal reflection. Detailed designs of the cathodes are proposed in the following sections to help solve these problems.

2 Structure of the chamber

The chamber is composed of a sandwich of two cathode planes surrounding a central anode wire plane, as shown in Fig. 1. Two epoxide resin frameworks and the cathodes seal the sensitive volume of the chamber, which avoids building a large gas box. A perfect electric shielding is realized by the copper layers at the cathodes which are connected to ground. To attain high positional resolution, it is desirable to minimize the anode-cathode distance (d), in particular to minimize the undesirable parallax dictated by

oblique tracks of secondary particles [6]. However, a small distance gives rise to problems relating to mechanical stability and tolerance. An anode-cathode distance (d) of 8 mm was selected for the purpose of getting a good planarity of the large chamber framework. The anode plane is made of 20 μm diameter gold plated tungsten wires, at a spacing of s=4 mm. Two thick protected wires (diameter: 75 μm and 100 μm) are introduced at each edge of the anode plane to make the electric edge filed uniform [7].

The signal processing of cathode X is shown in Fig. 2. The anode wires are connected together to give a common start signal for a time-to-digital converter (TDC). The positive pulses at each end of the delay line are amplified and discriminated by two constant fraction discriminators (CFD). The time intervals between the discriminator pulses and the common gate pulse are recorded by two channels of the TDC. The one dimensional coordinate of the impact position is reconstructed by the difference of the two time intervals. The electronics is totally the same at cathode Y, but the cathode strips are parallel to the anode wires, giving another dimensional coordinate.
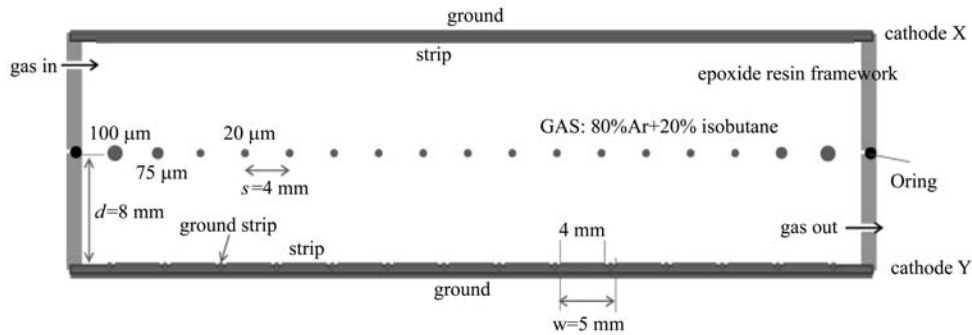

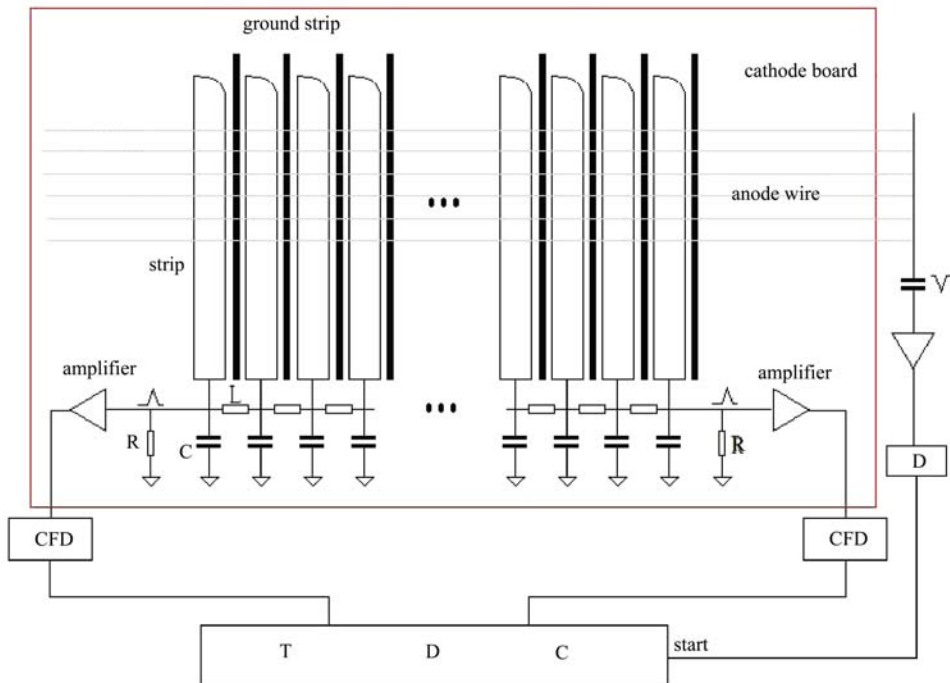Fig. 1.   The cross-sectional view of the chamber (perpendicular to the anode wire).

Fig. 2.   The scheme of the signal processing for the chamber.

3   Design of cathode plane

From the view of noise, a delay line with high characteristic impedance and a large delay time would be the best choice to get a good position resolution [8]. But the total delay time should be limited by the range of the TDC. Moreover the detector capacitance and the delay line impedance will act as a differentiating circuit (R-C circuit) to the avalanche signal seen at the cathode, which will change the leading edge of the signal Given this, a commercial tapped delay line chip 1507-50C was selected as the delay line. The chip has ten delay taps with a delay time of 5 ns per tap. The characteristic impedance of the delay line is 200 Ω. The principle of each delay cell is known in Fig. 3.
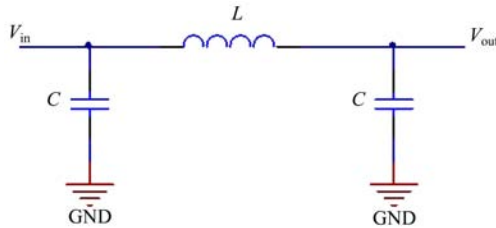

Fig. 3.   A cell of the delay line circuit. $L \approx 1$ μH and $C \approx 25$ pF, for the delay line chip 1507-50C.

The delay time per cell can be calculated by Formula (1) [9].

$$\tau = \frac{1}{\omega}\left[\frac{\omega}{\omega_0} + \frac{1}{3}\left(\frac{\omega}{\omega_0}\right)^3 + \ldots\right] \approx \frac{1}{\omega_0}, \quad (\omega \ll \omega_0),$$

$$\omega_0 \approx \frac{1}{\sqrt{LC}}, \tag{1}$$

$$Z_0 \approx \sqrt{\frac{L}{C}},$$

where ω is the frequency of the input signal, ω_0 is the cut-off frequency of the delay line, and Z_0 is the characteristic impedance of the delay line.

In the delay line readout, the optimum number of strips catching the signal is about 3. The distribution of the induced charge on the cathode plane is as wide as 1.58 d (FWHM). So the 5 mm strip pitch is selected, with 4 mm strip width and 1 mm separation. From the theoretical calculations for this design, the capacitance (C_s) between the adjacent strips and the capacitance (C_g) between the strips and ground is 19.4 pF/m and 95.6 pF/m respectively, which will lead to a 9.5% near end crosstalk at the adjacent

strips. As the crosstalk is dominated by the ratio of the capacitances mentioned above, a ground strip with a width of 0.4 mm was planted between the adjacent strips, shown in Fig. 2. The capacitances were changed to 8.9 pF/m and 141.3 pF/m, and the near end crosstalk was reduced to 3.7%

As the strip is coupled to the delay line directly, the capacitance (C_g) between the strip and the ground is parallel with the capacitance (C) in the delay cell. The cathode strips have a length of 325 mm, so C_g is about 46 pF, nearly two times of C(25 pF). From Formula (1), the time delay between two adjacent strips will be larger than 5 ns. Every two adjacent strips and the delay tap in the delay chip will form a new delay cell. To consider the signal transmission in these new delay cells, the model of the cathode strips is constructed in transmission line simulation software Q2D Extractor and exported to Simplorer. A triangular negative signal (with a rise time of 50 ns and a fall time of 150 ns, as shown in Fig. 4) is injected into a strip and the time delay of the signal arriving at other strips is recorded. A linear relationship between the time delay and the number of delay cells is shown in
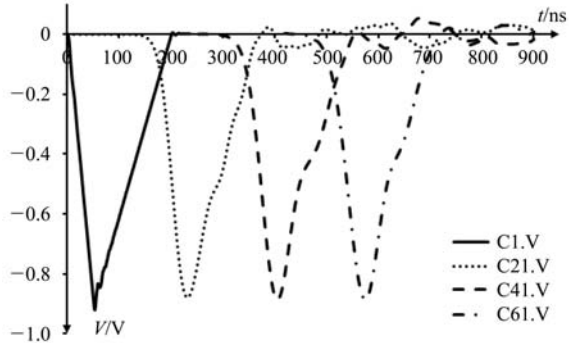

Fig. 4.   The signals delayed by a different number of delay units. C1.V is the initial injected signal. C21.V, C41.V and C61.V are the signals delayed by 20, 40 and 60 delay cells, respectively.
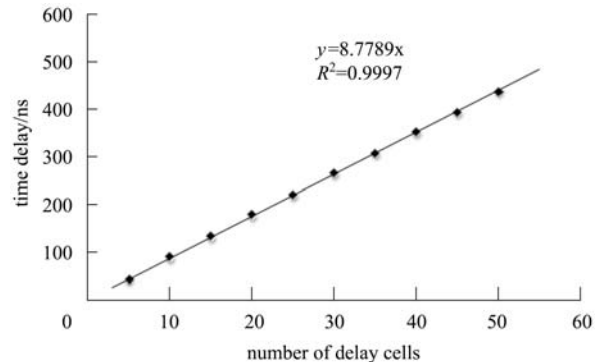

Fig. 5.   The relationship between the number of delay cells and the time delay.

Fig. 5. The time delay between each two adjacent strips is about 8.78 ns. So the cut-off frequency of the total delay circuit is 110 MHz, which is much larger than the frequency of the signal.

Moreover, the characteristic impedance of the new delay cell is no longer 200 Ω. A clear reflection signal was observed in the oscilloscope when terminated with a 200 Ω resistor. The reflection coefficient ρ can be defined as the ratio of the reflected voltage V_r and the original voltage V_0:

$$\rho = V_r/V_0 = (R-Z)/(Z+R), \qquad (2)$$

where Z is the characteristic impedance of the delay line, and R is the impedance of the matched resistor. The reflection coefficient is about 0.25, as shown in

Fig. 6(a). So the characteristic impedance of the delay circuit is 120 Ω. No significant reflections are observed in the oscilloscope when the signal readout line is terminated with a 120 Ω resistor (See Fig. 6(b)).

A voltage amplifier is equipped on the cathode to amplify the positive voltage pulse at the matched resistor R. The schematic diagram of the amplifier is shown in Fig. 7. The amplifier is composed of two operation amplifier stages. At the first stage, the operation amplifier works in the non-inverting mode. While at the second stage, the polarity of the signal is inverted. The total voltage gain of the amplifier is $(1+R_{FB1}/R_{FF1})*(-R_{FB2}/R_{FF2}) \sim -280$, with an input noise of 3.8 nV/(Hz)$^{1/2}$.

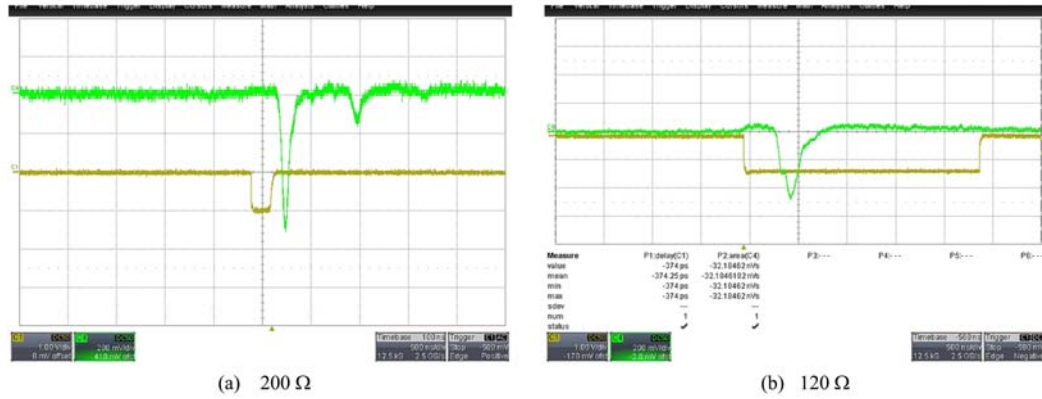(a)   200 Ω (b)   120 Ω

Fig. 6. Signal reflection of different matched resistance. The signals in (a) and (b) have been amplified by the voltage amplifier.
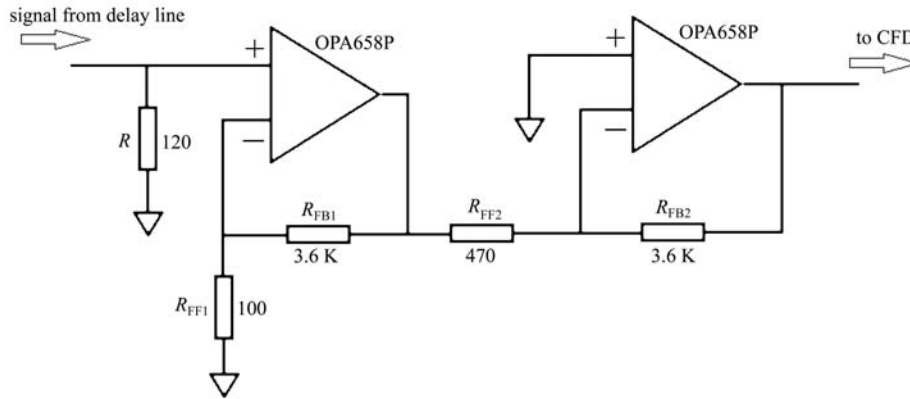

Fig. 7. Scheme of the amplifier.

4   Performance of the detector

A mixture of Ar and isobutane gases (80% Ar, 20% isobutane) were selected as the work gases because of the high gas gain. The chamber works at the

high voltage of 3020 V. Since the chamber does not have a thin window allowing the X-rays to penetrate, 59 keV gamma-rays from an Am-241 source with a collimator of 2 mm in diameter are used to calibrate the chamber. The calibration coefficient can be described in Formula (3).

$$x = K_x(t_{x1} - t_{x2}),$$

(3)

$$y = K_y(t_{y1} - t_{y2}),$$

where x and y are the coordinates of the source, t_{x1}, t_{x2}, t_{y1} and t_{y2} are the time intervals measured in the corresponding TDC channels. The calibration curve of the chamber is shown in Fig. 8. The calibration coefficients of two directions are almost the same, both about 0.28 mm/ns. So the real delay time per cell is $\tau =$ (5 mm/0.28 mm/ns)/2=8.9 ns, which is a good agreement with the simulation. Because of the bad collimation and the wide distribution of the excited and scattered electrons in the chamber, photons with energy of 59.5 keV are not suitable for the position resolution calibration.

A print board circuit with 1.5 mm diametric drills was introduced to replace the cathode Y to get the position resolution along the anode wires. The distance of 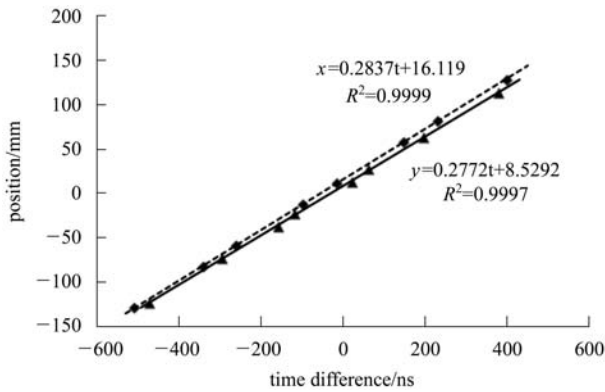two 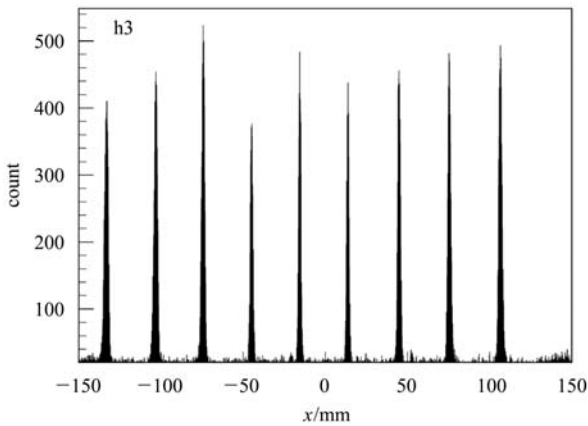adjacent drills is 3 cm. A Fe-55 source was placed on the drills to reconstruct the impact positions of the 5.9 keV X-rays (Fig. 9). The best position resolution along the anode wire is σ=670 μm (shown in Fig. 10), however considering the drill size contribution to the error, the position resolution is corrected to $\sigma_x = \sqrt{\sigma^2 - \left(1.5 \text{ mm}/\sqrt{12}\right)^2} \approx 510$ μm. The position resolution of the total chamber is shown in Fig. 11. The position resolution in the center of the chamber is the best, while at the two edges this parameter turns worse. Nevertheless, a position resolution below 1 mm can be obtained along the anode wires in the whole sensitive area. As the avalanche points are limited to the nearby surface of anode wires, the position resolution across the anode wire (y coordinate) is $\sigma_y = s/\sqrt{12}$=1.15 mm.
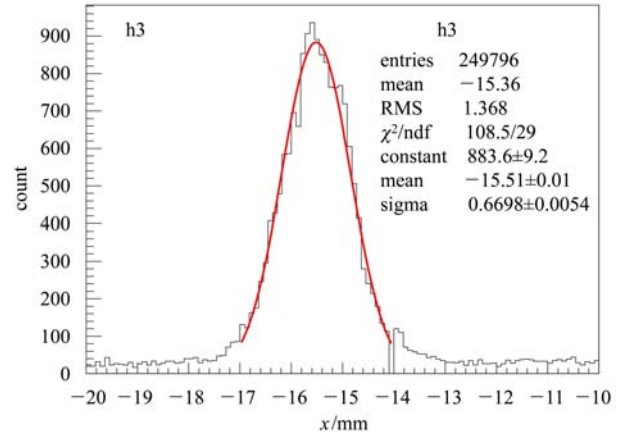

Fig. 8.   Calibration curve of the chamber.

Fig. 10.   The position resolution along the anode wire.

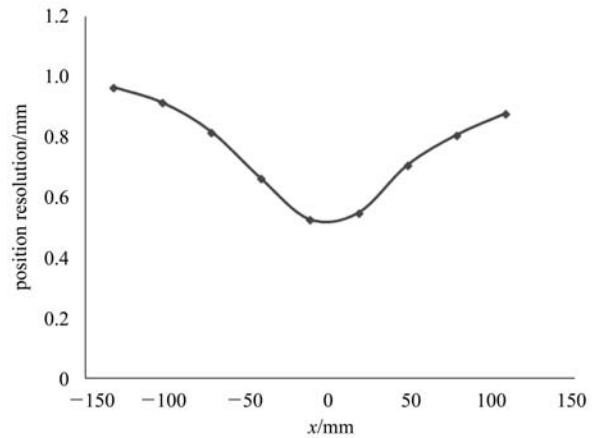Fig. 9.   The reconstructed positions of 5.9 keV X-rays at the direction of x coordinate.

Fig. 11.   The total position resolution of the chamber. In the center, the chamber has the best position resolution of 510 μm, while at the two edges, the position resolutions degrade to 1 mm.

5   Summary

A large area MWPC with delay line readout has been shown in this article. By adding a ground wire between the cathode strips and changing the matching resistance, we have solved the problem of signal crosstalk and reflections at the cathodes. A position resolution of less than 1 mm is obtained in the whole sensitive area of the chamber, while the position resolution in the center of the chamber could be less than 510 μm. The reason for the resolution to turn worse at the edge may be the dispersion of the signal when the signal is transported through the delay line, because at each edge of the chamber, the signal from the other side will pass through the maximum number of delay cells. It means that more elements should be considered when trying to construct a delay wire chamber larger than 30 cm×30 cm.

References

1　Charpak G, Bouclier R, Bressani T et al. Nucl. Instrum. Methods, 1968, **62**(3): 262
2　Boie R A, Fischer J, Inagaki Y et al. Nucl. Instrum. Methods, 1982, **201**(1): 93
3　http://sl.web.cern.ch/SL/Publications/bi98-023.pdf
4　HAN Li-Ying, LI Qi-Te, Faisal Q et al. Chinese Physics C (HEP & NP), 2009, **33**(5): 364
5　Beardsworth E, Fischer J, Iwata S et al. Nucl. Instrum. Methods, 1975, **127**(1): 29
6　Heiz A A, Filthuth W. United States Patent, 4965861.1990
7　WANG Xiao-Hu, ZHU Qi-Ming, CHEN Yuan-Bo et al. Chinese Physics C (HEP & NP), 2008, **32**: 903
8　Radeka V. IEEE Trans. Nucl. Science, 1974, **21**(1): 51
9　Guedes G P, Breskin A, Chechik R et al. Nucl. Instrum. Methods A, 2003, **513**(3): 473